NASA TECHNICAL NOTE

NASA TN D-5305

C. 1

NASA TN D-5305

RESEARCH AND DEVELOPMENT IN NEEDLE AND SLIT COLLOID THRUSTERS

by Kenneth W. Stark and Allan Sherman

Goddard Space Flight Center
Greenbelt, Md.

NATIONAL AERONAUTICS AND SPACE ADMINISTRATION • WASHINGTON, D. C. • FEBRUARY 1970

RESEARCH AND DEVELOPMENT IN NEEDLE AND SLIT COLLOID THRUSTERS

By Kenneth W. Stark and Allan Sherman

Goddard Space Flight Center
Greenbelt, Md.

NATIONAL AERONAUTICS AND SPACE ADMINISTRATION

For sale by the Clearinghouse for Federal Scientific and Technical Information
Springfield, Virginia 22151 – CFSTI price $3.00

ABSTRACT

A thorough test program was conducted to obtain familiarity with and proficiency in capillary needle colloid thruster technology. This technology is basically a means by which electrostatic particle spraying can be achieved through the use of slightly conductive propellants and high voltages. Forty-eight single needle tests were run with various needle materials and geometries, using several propellant combinations. Several test facility variations were employed to study secondary electron effects. From the results of these tests, an optimum configuration of needle material, needle geometry, propellant composition, needle-to-collector distance and high voltage to be used was obtained.

During this time two slit colloid thruster sources were designed and built. After the single needle testing was terminated, the annular slit thruster was tested successfully. Future efforts will concentrate on continued testing of the annular slit thruster to perfect its overall performance.

CONTENTS

RESEARCH AND DEVELOPMENT IN NEEDLE AND SLIT COLLOID THRUSTERS

by
Kenneth W. Stark and Allan Sherman
Goddard Space Flight Center

INTRODUCTION

For approximately 8 years various groups have conducted research and development in the field of electrostatic charged particle (colloid) propulsion. Briefly, colloid thrusters operate by the electrostatic spraying of liquids. The propellant, a low vapor pressure moderately conductive liquid, is sprayed from the rims of metallic capillary needles or slits that are maintained at high electric potential; this potential imparts a force on the liquid interface, causing the expulsion of very small charged particles. The very low power required for this charged particle formation is the feature making colloid thrusters competitive with ion engines, especially at thrust levels below 1 millipound.

Since the early reports on single needle colloid thruster tests (References 1 and 2), significant advances have been made in colloid needle-type thruster research and development. Multiple needle module test runs on the order of 1000 consecutive hours at 800 seconds specific impulse (Reference 3) and a 50-hour test on a 73-needle bipolar array (Reference 4) have been reported.

Because of this initial emphasis on needle-type thrusters, relatively little has been accomplished in developing single units of one flow area capable of producing high thrusts. The ultimate purpose of the program described herein is to conduct research and development in this area, resulting in single high thrust units whose inherent simplicity would offer obvious advantages over multiple needle arrays. First, a series of single needle tests was run in order to gain familiarization with colloid thruster operation and testing techniques and to gain knowledge that could be used in designing the advanced geometry. Along with this needle testing, an analytical study of the colloid dispersion process was conducted.* This report describes the overall test procedure, the apparatus used, and the needle testing results. The data reduction program employed and a complete presentation of the design and testing of the new single high-thrust unit (annular slit) are summarized.

*Unpublished NASA Document, Sherman, A., "Parametric Analysis of Electrostatic Dispersion of a Liquid," GSFC X-734-67-321, 1967.

DATA REDUCTION

Before proceeding with the discussion of the results of this program, it is appropriate to describe the method by which the performance of these thrusters is evaluated. The optimum procedure for testing and evaluating thruster performance would be to use a direct thrust measurement system and an absolute flow measuring device. Unfortunately, suitable means for directly measuring thrust and flow rates for these experimental laboratory models are not available at this time.

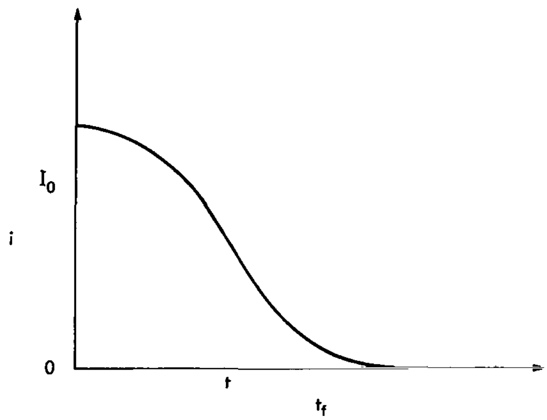

Figure 1—Typical time of flight trace.

Present data-reducing methods use techniques developed early in the history of colloid thruster technology (References 1 and 3). One method employs the time of flight (TOF) trace, which is numerically integrated to yield thrust, specific impulse, charge to mass ratios, efficiency, mass flow rates, and average particle velocity.

A TOF trace is obtained by simultaneously grounding the needle voltage and recording the current decay curve caused by the particles in flight after grounding. A typical TOF curve is shown in Figure 1.

A computer program was written for the reduction of data obtained from the TOF curves, which computes the colloid thruster performance parameters from input sets of points, current, and time. These points are obtained from enlarged photographs (8 in. × 10 in.) of the original oscilloscope picture (3 in. × 5 in.).

The sets of points used in the program evaluate numerically the following two integrals required for the TOF equations:

$$X_1 = \int_0^{t_f} i\,dt\ ; \tag{1}$$

$$X_2 = \int_0^{t_f} it\,dt\ . \tag{2}$$

The numerical method selected for the evaluation of these integrals is Simpson's 1/3 rule. Hence

$$X_1 = \frac{\Delta t}{3}\left[i_0 + 4i_1 + 2i_2 + 4i_3 + 2i_4 + \cdots 4i_{N-1} + i_N\right] + \text{error term}\ ; \tag{3}$$

and

$$X_2 = \frac{\Delta t}{3}\left[i_0 t_0 + 4i_1 t_1 + 2i_2 t_2 + 4i_3 t_3 + 2i_4 t_4 + \cdots 4i_{N-1} t_{N-1} + i_N t_N\right] + \text{error term} , \tag{4}$$

where N should be an even number.

The error involved in the above calculations was evaluated in the following way. First, the integral for a typical TOF trace was carried out using the above equations with both 11 and 19 sets of points. Second, the same calculation was performed using the generally less accurate Trapezoid Rule to evaluate the integral numerically. The results of these calculations for X_1 are summarized in Table 1.

Table 1

Comparison of Numerical Integration Methods.

Method	11 Points	19 Points	Percent Difference
Simpson	14.827	14.827	0
Trapezoid	14.880	14.840	.27
Percent difference	.36	.086	

In both of the cases shown in Table 1, the negligible change in the value of X_1 in increasing N from 11 to 19 shows that the error terms in Equations 3 and 4 are extremely small for $N \geq 11$. Similarly, the close agreement between the results obtained by the Trapezoid's and Simpson's Rules show that the error in using either method for $N \geq 11$ is negligible. Since similar results were also obtained for the computation of X_2, and since for the data reported herein the minimum number of point sets was 13, it can be concluded that X_1 and X_2 are computed to a high degree of accuracy by the data reduction program.

Once X_1 and X_2 are calculated, the program then computes the test performance parameters by the standard TOF equations:

$$T = \frac{2V}{d} X_1 ; \tag{5}$$

$$m = \frac{4V}{d^2} X_2 ; \tag{6}$$

$$ACMR = \frac{I_c}{m} ; \tag{7}$$

$$\eta = \frac{T^2}{2VI_c m} ; \tag{8}$$

$$\eta_b = \frac{q/m}{ACMR} ; \tag{9}$$

and

$$I_{sp} = \frac{T}{mg_0} . \tag{10}$$

Symbols used here and elsewhere in this report are defined in the List of Symbols at the end of the text.

LABORATORY APPARATUS AND PROCEDURE

Testing of the colloid thrusters must be conducted in a vacuum environment for two reasons. First, the voltage necessary to operate the various configurations could range from 6 to 25 kv; with these high voltages and the thin-rimmed firing edges used, corona discharges would likely occur in air. Second, in air the high velocity particles would experience drag effects which would lead to erroneous TOF results.

Figure 2 shows the basic vacuum chamber setup used, with the needles and collector in a horizontal firing position. When the annular slit testing began, it was necessary to assume the vertical position in order to lessen the effect of gravity on the meniscus and beam trajectory. However, the test procedure and operation is the same for both the vertical and horizontal arrangements and is as follows:

After each propellant combination is mixed, and before each run, the propellant is degassed under vacuum conditions. This is to assure that air and other higher vapor pressure contaminants (e.g., water) are removed; if this is not done, erratic performance and corona will result during operation. For this procedure the propellant feed tube is raised above the level of propellant and clamped at point 6. The propellant is then heated and stirred while the vacuum pump (4) is operating. The Pirani vacuum gauge is used to monitor the pressure. During this procedure valve 1 is open and valve 2 is closed. After degassing is completed, the propellant is cooled to room temperature, the clamp (6) is removed, the feed tube is inserted into the propellant, valve 1 is closed, and the vacuum pump (4) is shut off. To initiate propellant flow, the vacuum pump (5) is

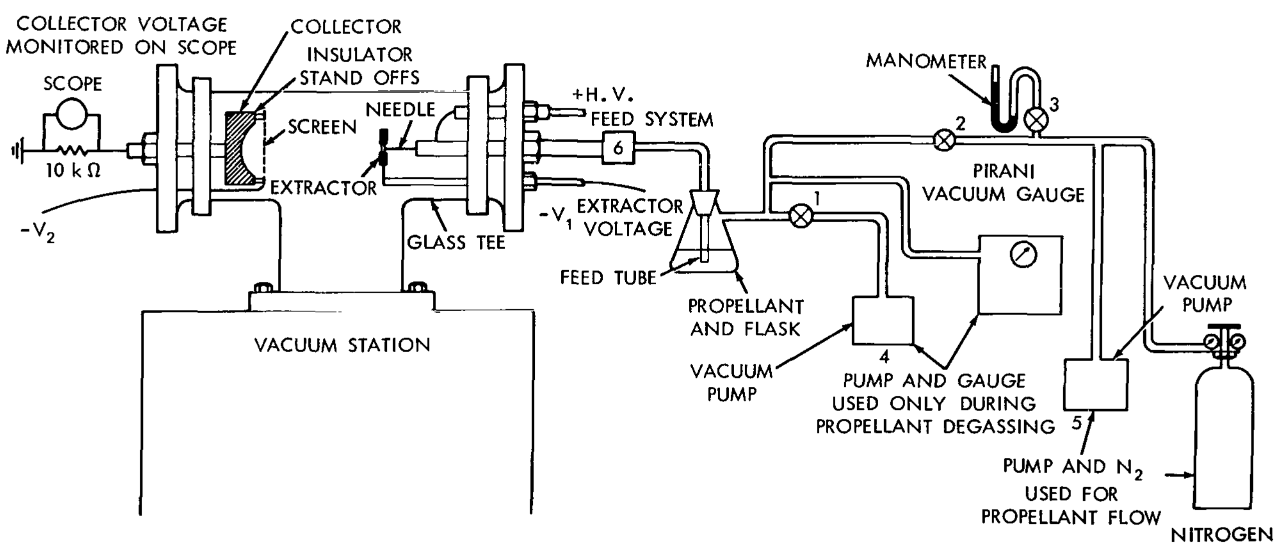

Figure 2—Vacuum chamber test setup.

turned on, valves 2 and 3 are opened and the nitrogen gas supply is turned on until the correct pressure differential is observed on the manomèter.

When the propellant reaches the firing surface of the needles or slits, high voltage is applied to the thruster. Negative voltages are applied to the extractor and screen. The charged particles expelled from the thruster impinge upon the collector, resulting in a current that flows through a resistor to ground. The voltage across this resistor is monitored on an oscilloscope and, from this, the diagnostic test procedures are conducted as described in a previous section. Figures 3 and 4 show schematic representations of the thruster voltage shorting (zapper) units used to

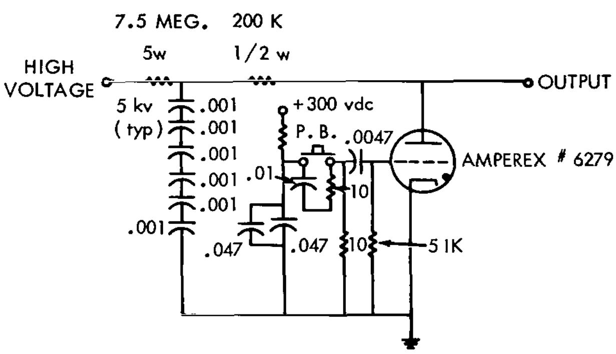

Figure 3—Thyratron zapper circuit.

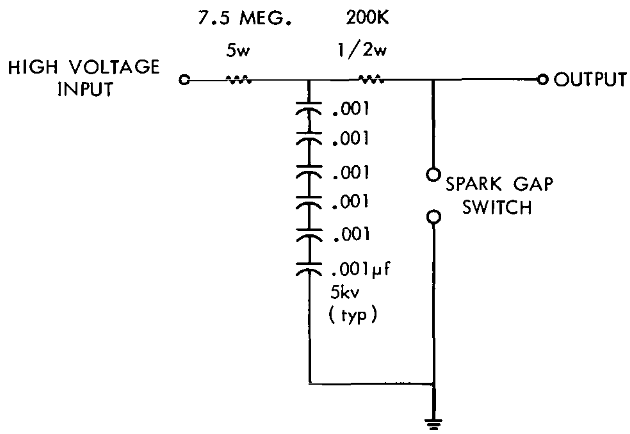

Figure 4—Ball zapper circuit.

obtain the TOF traces. As mentioned previously these units accomplish the dual purpose of simultaneously grounding the thruster voltage and triggering the scope to register the current of all particles in flight at the moment of the grounding.

CAPILLARY NEEDLE TEST PROGRAM

Before pursuing the main goal of the colloid thruster program—developing a high thrust high performance slit thruster—it was necessary to conduct a familiarization program centered on the already existing capillary needle technology. Forty-eight needle tests were run in this program. As well as performing the familiarization function, these tests provided an opportunity to study the performance of different propellants, the effect of variations in extractor size and potential on performance, the effect of shield and screen voltages on secondary electron emission, and the performance of different needle tip geometries. An investigation to determine what needle material would minimize the tip erosion caused by the combination of high voltage, vacuum conditions and electrolytic propellants was also carried out.

A summary of the significant needle testing results is presented in Table 2.

Table 2

Summary of Single Needle Tests.

Test Number	Purpose of Test	Needle	Propellent	P_f (mm Hg)	V_N (volts)	V_{EXT} (volts)	V_{SCR} (volts)	I_C (μamps)	I_N (μamps)
13P	General testing of Hastelloy C needle	Hastelloy C	NaI (20g)/ Glyc. (100 ml)	160	6000	− 500	−45	.79	
14P	General testing of Hastelloy C needle	Hastelloy C	NaI (20g)/ Glyc. (100 ml)	160	6000	− 500	−45	.62	
15P	General testing of Hastelloy C needle	Hastelloy C	NaI (20g)/ Glyc. (100 ml)	160	6000	− 500	−45	.68	
16P	General testing of Hastelloy C needle	Hastelloy C	NaI (20g)/ Glyc. (100 ml)	160	6000	− 500	−45	.55	
17P	General testing of Hastelloy C needle	Hastelloy C	NaI (20g)/ Glyc. (100 ml)	160	6000	− 500	−45	.73	
18P	General testing of Hastelloy C needle	Hastelloy C	NaI (20g)/ Glyc. (100 ml)	160	6000	− 500	−45	1.0	
19P	General testing of Hastelloy C needle	Hastelloy C	NaI (20g)/ Glyc. (100 ml)	160	6000	− 500	−45	.82	
20P	To determine the effect of screen voltage on steady state values and TOF results	Hastelloy C	NaI (20g)/ Glyc. (100 ml)						
1.				153	5900	− 473	−22	.87	2.2
2.				153	5900	− 473	−45	.63	1.62
3.				153	5900	− 473	−67	.55	1.99
4.				153	5900	− 473	−90	.53	1.90
5.				153	5900	− 473	Ground	1.27	2.8
6.				153	5900	− 473	−45	.70	2.45
21P	To determine the effect of screen stand-off distance on steady state values and TOF results	Platinum	NaI (20g)/ Glyc. (100 ml)						
1.				110	7100	− 473	Ground	2.14	6
2.				110	7100	− 473	−45	.70	5.8
3.				110	7100	− 473	−67	.67	5.65
4.				110	7100	− 473	−90	.65	5.9
5.				110	7100	− 473	−22	.79	5.65
22P	Rerun of 21P but with glass feed system	Platinum	NaI (20g)/ Glyc. (100 ml)						
1.				112	7850	− 473	−22	.87	7.1
2.				112	7850	− 473	−45	.72	6.85
3.				112	7850	− 473	−67	.58	6.85
4.				112	7850	− 473	−90	.48	6.95
5.				112	7850	− 473	Ground	3.85	7.8
6.				112	7850	− 473	Floating	5.2	6.7
7.				112	7850	− 473	Floating	4.23	
23P	Rerun of 20P but with platinum needle and same P_f and V_N as 22P	Platinum	NaI (20g)/ Glyc. (100 ml)						
1.				115	7850	− 473	−22	1.43	5.4
2.				115	7850	− 473	−45	1.61	5.5
3.				115	7850	− 473	−67	1.01	5.3
4.				115	7850	− 473	−90	1.01	5.4
5.				115	7850	− 473	Ground	1.13	4.95

I_{EXT} (μamps)	ACMR (coul/kg)	I_{SP} (sec)	m (lbm/sec)	$\frac{I_N}{I_C}$ m (lbm/sec)	T (μlb)	$\frac{I_N}{I_C}$ T (μlb)	η_b (%)	q/m (coul/kg)	Comments
	2641	540.2	$.66 \times 10^{-9}$		.356		89.2	2356	Data for 13P → 19P were obtained during continuous run of Hastelloy C needle for 25-1/2-hour period.
	2917	546.0	$.47 \times 10^{-9}$		.257		83.8	2444	
	4163	654.3	$.36 \times 10^{-9}$		.236		83.0	3455	P_f was reduced to 60 mm Hg for 15-1/2 hours (overnight).
	3698	608.0	$.33 \times 10^{-9}$		.201		82.1	3036	I_c was basically stable but shifted periodically and showed some evidence of sparking.
	3998	600.0	$.40 \times 10^{-9}$		.240		71.5	2859	Erosion of the needle occurred but was smoother than with stainless needle.
	3652	553.0	$.60 \times 10^{-9}$		.332		67.0	2447	
	3074	489.3	$.59 \times 10^{-9}$		.289		62.9	1934	
1.89×10^{-2}	1329	330.1	1.44×10^{-9}	3.64×10^{-9}	.476	1.20	67.3	894	Screen stand-off distance 1 inch
1.89×10^{-2}	1004	282.3	1.38×10^{-9}	3.54×10^{-9}	.390	1.00	65.2	655	
1.25×10^{-2}	1092	305.4	1.11×10^{-9}	4.02×10^{-9}	.339	1.23	70.1	765	
2.5×10^{-2}	924.8	274.5	1.26×10^{-9}	4.51×10^{-9}	.347	1.24	67.0	620	
2.65×10^{-2}	1476	340.0	1.9×10^{-9}	4.19×10^{-9}	.646	1.42	64.5	952	
2.25×10^{-2}	996.3	286.6	1.55×10^{-9}	5.43×10^{-9}	.444	1.55	67.7	674	
.55	2240	476.7	2.11×10^{-9}	5.91×10^{-9}	1.0	2.80	69.2	1550	Screen stand-off distance 1/4 inch
.52	1677	416.6	$.92 \times 10^{-9}$	7.63×10^{-9}	.383	3.17	70.6	1184	
.45	1693	425.4	$.87 \times 10^{-9}$	7.34×10^{-9}	.371	3.13	72.9	1234	
.51	1935	444.6	$.74 \times 10^{-9}$	6.71×10^{-9}	.329	2.98	69.7	1349	
.45	1739	431.0	1.0×10^{-9}	7.15×10^{-9}	.431	3.08	72.8	1266	
.2									All glass feed system
.2									
.18									Positive overshoot on all but floating point test.
.22									
.26									Screen stand-offs 1/4 inch
.68									
	2014	422.0	4.63×10		1.95		54.4	1096	
.08	1382	422.1	2.28×10^{-9}	8.61×10^{-9}	.96	3.62	79.6	1100	Screen stand-off distance 1 inch
.07	2008	484.8	1.77×10^{-9}	6.05×10^{-9}	.857	2.93	72.3	1452	Collector current fairly steady.
.07	1462	438.1	1.52×10^{-9}	7.97×10^{-9}	.667	3.50	81.1	1186	Positive overshoot on all but
.068	1759	483.4	1.27×10^{-9}	6.80×10^{-9}	.612	3.27	82.0	1442	Test #2.
.07	879	342.7	2.83×10^{-9}	12.4×10^{-9}	.971	4.26	82.5	725	

Table 2 (continued)

Test Number	Purpose of Test	Needle	Propellent	P_f (mm Hg)	V_N (volts)	V_{EXT} (volts)	V_{SCR} (volts)	I_C (μamps)	I_N (μamps)
24P	To determine the effect of operating with a metal screen liner in vacuum T	Platinum	NaI (20g)/ Glyc. (100 ml)	108	7900	− 473	−22		
25P	Duration run for platinum needle	Platinum	NaI (20g)/ Glyc. (100 ml)	107	8200	− 473	−22		
26P	To determine the effect of varying the concentration of NaI solution	Platinum	NaI (10g)/ Glyc. (100 ml)						
1.				103	8650	− 473	−22	.09	.31
2.				103	8650	− 473	−45	.09	
3.				103	8650	− 473	−67	.09	
4.				103	8650	− 473	−90	.08	
5.				103	8650	− 473	Ground	.10	
27P	To determine the effect of varying the concentration of NaI solution	Platinum-10% Iridium	NaI (15g)/ Glyc. (100 ml)						
1.				110	8000	− 473	−22	.05	2.4
2.				110	8000	− 473	−45	.05	2.3
3.				110	8000	− 473	−67	.05	2.5
4.				110	8000	− 473	−90	.05	2.3
5.				110	8000	− 473	Ground	.05	2.4
28P	To determine the effect of varying the concentration of NaI solution	Platinum-10% Iridium	NaI (18g)/ Glyc. (100 ml)						
1.				98	9000	− 473	−22	.65	
2.				98	9000	− 473	−45	.56	
3.				98	9000	− 473	−90		
29P	Test hydrochloric acid as propellent	Platinum-10% Iridium	HCl (2.5 ml)/ Glyc. (100 ml)	107	8000	− 473	−22	.60	
30P	Test hydrochloric acid as a propellent	Platinum-10% Iridium	HCl (34 ml)/ Glyc. (100 ml)						
31P	Test sulphuric acid as a propellent	Platinum-10% Iridium	H_2SO_4 (10-1/2 ml)/ Glyc. (100 ml)						
32P	Test sulphuric acid as a propellent	Platinum-10% Iridium	H_2SO_4(2 ml)/ Glyc. (250 ml)						
33P	Test sulphuric acid as a propellent	Platinum-10% Iridium	H_2SO_4(2 ml)/ Glyc. (250 ml)	245	8700	− 473	−90	.48	
34P	Test sodium hydroxide as a propellent	Platinum-10% Iridium	NaOH (1g)/ Glyc. (100 ml)	230	9200	− 473		.45	

I_{EXT} (μamps)	ACMR (coul/kg)	I_{SP} (sec)	m (lbm/sec)	$\frac{I_N}{I_C}m$ (lbm/sec)	T (μlb)	$\frac{I_N}{I_C}T$ (μlb)	η_b (%)	q/m (coul/kg)	Comments
									Very erratic. Test terminated. 1/4-inch stand-off distance from this point on.
									Same needle as in 22P, 23P, 24P
									Operating conditions varied from those listed.
									Ran smoothly for one day; was spiking next day. Argon ran out third day.
.1	93.97	124.1	2.1×10^{-9}	7.25×10^{-9}	.262	.904	91.78	86.25	Very stable operation
.1	98.58	125.8	2.0×10^{-9}		.252		89.21	87.94	
.1	95.43	121.8	2.1×10^{-9}		.253		87.11	83.13	
.1	87.94	123.3	2.0×10^{-9}		.247		96.84	85.16	
.1	99.66	121.2	2.2×10^{-9}		.268		82.49	82.21	
.11	78.19	114	1.41×10^{-9}	67.6×10^{-9}	.161	7.72	100.	78.66	Very stable operation
.11	80.95	115.8	1.36×10^{-9}	62.6×10^{-9}	.158	7.27	100.	81.19	
.11	78.19	114	1.41×10^{-9}	70.5×10^{-9}	.161	8.05	100.	78.66	
.11	78.19	114	1.41×10^{-9}	64.9×10^{-9}	.161	7.41	100.	78.66	
.11	76.3	112.6	1.45×10^{-9}	69.5×10^{-9}	.163	7.82	100.	76.83	
.19	1468	447.4	$.98 \times 10^{-9}$		.437		73.4	1078	Very erratic performance
.19	1799	481.0	$.69 \times 10^{-9}$		.332		70.4	1266	Test terminated
.25									
	71.63	109.1	1.85×10^{-9}		.202		100.	72.13	Started stable but became very erratic. Bubbles observed at needle inlet.
									Very erratic performance at + and − V_N. Severe needle erosion.
									Very erratic with erosion of needle. Ran with both positive and negative V_N.
									Very erratic with some erosion of needle. Propellent not completely degassed.
	246.3	204.8	4.3×10^{-9}		.88		94.8	233.4	Erratic performance; no needle erosion
	208.3	181.1	4.76×10^{-9}		.863		82.94	172.8	Fairly stable performance

Table 2 (continued)

Test Number	Purpose of Test	Needle	Propellent	P_f (mm Hg)	V_N (volts)	V_{EXT} (volts)	V_{SCR} (volts)	I_C (μamps)	I_N (μamps)
35P	Test sodium hydroxide as a propellent	Platinum-10% Iridium	NaOH (2.3g)/ Glyc. (100 ml)						
1.				157	4900	− 473	−22	.30	
2.				193	4900	− 473	−22	.52	
3.				195	5000	− 473	−22	.28	
4.				105	5400	− 473	−22	.39	
5.				105	5900	− 473	−22	.59	
6.				60	6000	− 473	−22	.52	
7.				35	6300	− 473	−90	.46	
36P 2.	Test sodium hydroxide propellent at high feed pressure	Platinum-10% Iridium	NaOH (2.3g)/ Glyc. (100 ml)	109	6000	− 473	−45	.15	
37P	Test sodium hydroxide propellent at low feed pressure	Platinum-10% Iridium	NaOH (2.3g)/ Glyc. (100 ml)						
1.				42	6800	− 473	−45	.15	
2.				40	6900	− 473	−45	.46	
38P	Test sodium iodide propellent at high and low pressures	Platinum-10% Iridium	NaI (20g)/ Glyc. (100 ml)						
1.				315	8400	− 473	−22	.50	
2.				33	9600	− 473	−22	.23	
39P	Test first inside tapered needle (I.T.N.)	Platinum-10% Iridium	NaI (20g)/ Glyc. (100 ml)						
1.				50	6200	− 473	−22 or −45	.49	
2.				175	7800	− 473	−22 or −45	1.95	
40P	Test effect of smaller diameter extractor (I.T.N.)	Platinum-10% Iridium	NaI (20g)/ Glyc. (100 ml)						
1.				53	6200	− 473	−22 or −45	.19	
2.				177	7800	− 473	−22 or −45	3.25	
3.				37	6700	− 473	−22 or −45	.75	
41P	Test effect of coating screen and rear assembly with aquadag (I.T.N.)	Platinum-10% Iridium	NaI (20g)/ Glyc. (100 ml)						
1.				43	7500	− 473	−22 or −45	.33	
2.				40	6700	− 473	−22 or −45	.31	
3.				175	7700	− 473	−22 or −45	1.09	
42P	Test effect of auxiliary plate on TOF overshoot (I.T.N.)	Platinum-10% Iridium	NaI (20g)/ Glyc. (100 ml)						
1.				40	6700	− 473	−22	.74	
2.				180	7600	− 473	−22	2.72	
43P	Retest of 39P (I.T.N.)	Platinum-10% Iridium	NaI (20g)/ Glyc. (100 ml)	42	8200	− 473	−45	.39	

I_{EXT} (μamps)	ACMR (coul/kg)	I_{SP} (sec)	m (lbm/sec)	$\frac{I_N}{I_C}m$ (lbm/sec)	T (μlb)	$\frac{I_N}{I_C}T$ (μlb)	η_b (%)	q/m (coul/kg)	Comments
	595.5	211.1	1.11×10^{-9}		.235		74.42	443.2	Fairly stable. Large amount of precipitate observed at needle tip after test. No apparent tip erosion.
	584.6	223.5	1.96×10^{-9}		.438		84.44	493.6	
	374.5	180.3	1.65×10^{-9}		.297		84.15	315.1	
	987.2	308.8	$.87 \times 10^{-9}$		.269		86.69	855.8	
	1390	370.6	$.94 \times 10^{-9}$		.347		81.13	1128	
	2009	452.3	$.57 \times 10^{-9}$		.258		82.24	1652	
	3350	590.0	$.30 \times 10^{-9}$		.177		78.0	2613	
	286.1	167	1.16×10^{-9}		.193		78.8	225.4	4-hour test. Some precipitate on needle but not as much as in 35P.
	772.7	300.0	$.43 \times 10^{-9}$		.129		83.3	643.7	4-hour test. Some precipitate on needle rim but not as much as in 35P.
	1879	474.7	$.54 \times 10^{-9}$		.256		84.2	1582	
	299.3	196.0	3.68×10^{-9}		.722		74.2	222.1	Erratic; precipitate on needle but not as much as 35P
	1293	410.0	$.39 \times 10^{-9}$		.160		65.2	843.0	
	1281	196.0	$.84 \times 10^{-9}$		.310		81.8	1048	Very steady at low pressure; somewhat unsteady at high pressure
	1907	450.3	2.25×10^{-9}		1.015		66.1	1261	
	2086	448.8	$.2 \times 10^{-9}$		.09		75.5	1575	Extractor size changed from 7/16 inch i.d. to .279 inch i.d.
	2703	592.8	2.65×10^{-9}		1.57		80.8	2184	Erratic performance
	2326	525.7	$.71 \times 10^{-9}$		.374		86.0	2000	Positive overshoot on TOF
	1110	338.1	$.66 \times 10^{-9}$		.22		66.5	738.2	Screen and rear assembly coated with aquadag. Positive overshoot occurred on TOF. .279 inch i.d. extractor; erratic performance
	992.7	333.0	$.69 \times 10^{-9}$		.23		84.7	840.8	
	680.5	276	3.53×10^{-9}		.97		70.4	479.1	
	2384	533.0	$.68 \times 10^{-9}$		.362		85.0	2026	Plate at needle potential located in back of needle assembly. Positive overshoot was eliminated, but effect of plate on field unknown; .279 inch i.d. extractor.
	2191	530.0	2.7×10^{-9}		1.43		80.1	1755	
	2694	604.9	$.32 \times 10^{-9}$		.193		80.3	2168	Screen and rear assembly coated with aquadag. Data indicated current leak between screen and collector. Large extractor (7/16 inch i.d.) very stable.

Table 2 (continued)

Test Number	Purpose of Test	Needle	Propellent	P_f (mm Hg)	V_N (volts)	V_{EXT} (volts)	V_{SCR} (volts)	I_C (μamps)	I_N (μamps)
44P	Retest of 39P (I.T.N.)	Platinum-10% Iridium	NaI (20g)/ Glyc. (100 ml)	38	7800	− 473	−45	.56	
45P	Test second inside tapered needle (I.T.N.)	Platinum-10% Iridium	NaI (20g)/ Glyc. (100 ml)	35	5500	− 473	−45	.29	
46P	Test effect of varying extractor voltage on performance (I.T.N.)	Platinum-10% Iridium	NaI (20g)/ Glyc. (100 ml)						
1.				57	7800	− 473	−45	.33	
2.				57	6300	− 780	−45	.39	
3.				57	6400	−1100	−45	.39	
4.				57	6400	−1450	−45	.41	
5.				57	6400	− 780	−90	.30	
47P 2.	Test effect of higher P_f on inside tapered needle performance	Platinum-10% Iridium	NaI (20g)/ Glyc. (100 ml)	90	7700	− 473	−45	1.23	
48P	To test outside-tapered needle	Platinum-10% Iridium	NaI (20g)/ Glyc. (100 ml)						
1.				89	8100	− 473	−45	.81	20
2.				95	7200	− 473	−45	1.2	16
3.				100	7000	− 473	−45	1.16	
4.				100	6000	− 473	−45		
5.				98	7300	− 473	−45	.80	15
6.				98	5900	− 473	−45	.59	5

I_{EXT} (μamps)	ACMR (coul/kg)	I_{SP} (sec)	m (lbm/sec)	$\frac{I_N}{I_C} m$ (lbm/sec)	T (μlb)	$\frac{I_N}{I_C} T$ (μlb)	η_b (%)	q/m (coul/kg)	Comments
	2888	601.0	$.43 \times 10^{-9}$		.259		79.2	2287	Same as 43P but without aquadag; very stable
	1474	368.0	$.43 \times 10^{-9}$		.158		78.8	1162	Erratic performance. Residue buildup at needle tip. Positive overshoot on TOF.
	989.2	356.1	$.74 \times 10^{-9}$		.262		79.6	787.4	Caked-up deposit around rim of needle
	1824	444.6	$.47 \times 10^{-9}$		.210		83.4	1521	
	1908	443.2	$.45 \times 10^{-9}$		.200		78.0	1488	
	1718	455.6	$.53 \times 10^{-9}$		.240		91.5	1572	
	2501	535.0	$.26 \times 10^{-9}$		.139		84.0	2101	
	5929	866.9	$.46 \times 10^{-9}$		.397		79.8	4731	Stable performance at P_f = 90 mm Hg
.48	6508	885.0	$.27 \times 10^{-9}$	6.67×10^{-9}	.239	5.90	69.7	4536	Performance not very stable at V_N = 8 kv. Stable performance at V_N = 6 kv.
.42	5243	823.0	$.5 \times 10^{-9}$	6.66×10^{-9}	.412	5.50	85.7	4493	
	4202	705.1	$.61 \times 10^{-9}$		.429		81.9	3441	
.4	3915	714.3	$.45 \times 10^{-9}$	8.45×10^{-9}	.322	6.05	86.5	3386	
.16	1331	368	$.98 \times 10^{-9}$	8.30×10^{-9}	.360	3.05	83.6	1113	

Factors Influencing Secondary Electron Emission and Performance

Secondary emission is one of the most difficult problems to evaluate in colloid testing. For example, secondary electron emission can occur at the collector, at the suppressor screen, at the end plates of the vacuum chamber, or at the needle assembly. In fact, because of the high energy of the colloid particles (on the order of 10^7 times the work function of most metals), it is conceivable that either the original colloid droplet or shattered fragments of the original droplet could initiate secondary electron emission at any metallic surface within the chamber. In addition, it is suggested by Beynon et al. (Reference 3) that these fragments, which result from shattering upon impact with the collector, might be able to maintain a positive charge. Thus "positive secondaries" may also be produced in the chamber.

Performance can be disturbed by many possible effects generated by secondary electrons. Three of the most prominent effects observed during this test program will be discussed.

The first and most difficult to interpret is positive overshoot of the TOF trace, as shown in Figure 5. A problem arises here in the reduction of the TOF trace data to obtain performance information. The positive overshoot of the TOF trace may be explained in terms of secondary emission effects. For example, assume that under steady state conditions the spray into the collector contains a substantial number of secondary electrons as well as the positively charged propellant droplets. After the zap, the rate of secondary electron emission decreases, as the higher velocity particles reach the collector. At the same time, the electrons in the beam, which are of higher velocity than the positive particles, are being reabsorbed either at the collector or elsewhere in the chamber. Hence there is a net rate of decrease of electrons in the beam. If this rate of decrease of negative charge is larger than the rate of decrease of positive charge that reaches the collector, an initial positive overshoot will occur. After a very short time, however, the secondary electron effect becomes negligible and the TOF assumes its usual shape.

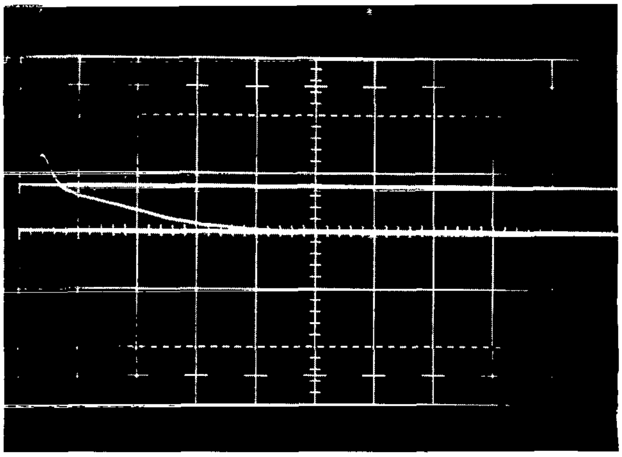

Figure 5—Positive overshoot on TOF trace.

It should be noted that, for those tests reported herein in which a positive overshoot occurred, the current was assumed for the purpose of calculations to be at the steady state value for the duration of the overshoot. This produces an error in the results. However, since the flow arrived at by reduction of the TOF data agreed generally (to within 20 percent) with the flow calculated by means of Poiseuille's equation, it is assumed that the other TOF data-reduced values are of reasonable accuracy.

Another problem area is "back bombardment" of the firing source by the secondary electrons. One reason for the presence of the extractor is to prevent this back bombardment; but, in spite of the extractor, a certain amount of back bombardment can occur. If it becomes significant, an error results in the needle current reading; the needle current assumes a value which is higher by the amount of secondary electrons absorbed. In addition, tar-like deposits have been reported (Reference 3), presumably caused by this back bombardment.

A third effect, difficult to determine experimentally, is erratic performance caused by back bombardment. It is possible that the back bombardment could disrupt the meniscus at the firing surface, causing unstable particle generation.

A thorough theoretical analysis of the secondary emission phenomena occurring within the vacuum chamber would be extremely complicated and, undoubtedly, of questionable validity. Therefore, this program included a series of tests whose goal was to determine what test operating conditions might lessen secondary effects, and, to some degree, what error in the final data is caused by the secondary emission effects. These tests were designated by the numbers 1P to 48P, where P stands for preliminary. All data were reduced from the TOF traces using the computer data reduction technique described earlier in this report.

Screen Voltage Variation

Tests 20P to 23P were conducted to determine the effects of screen voltage and screen distance from the collector on secondary electron emission.

During test 20P, all operating conditions were held constant, except suppressor screen voltage. This same procedure was then followed for test 21P, except that the screen stand-off distance was reduced from 1 inch to 1/4 inch. Figures 6 and 7 show the various currents and other performance parameters, as computed from the TOF curves versus suppressor screen voltage for tests 20P and 21P.

For both tests, the collector current decreases as the suppressor voltage becomes more negative. Thus the net flow of electrons from the collector decreases, and it is reasonable to assume that this decrease is due to suppression of secondary electrons initiated at the collector. It is also interesting to note that with the 1/4-inch stand-off distance (test 21P), the final value of collector current is reached at a lower absolute value of negative voltage.

In both tests 20P and 21P, the screen current increases as the screen potential becomes more negative, indicating that this increase can be caused by a combination of an increase in the net flow of electrons from the screen and an increase in the number of positive particles hitting it. It is reasonable to assume that part of this higher net electron flow from the screen is due to the suppression of the secondary electrons from the collector which would otherwise come back to the screen.

It should also be noted from Figures 6 and 7 that, when both the screen and collector are grounded, their currents are about equal. This is as expected because the transmissivity of the screen is about 50 percent.

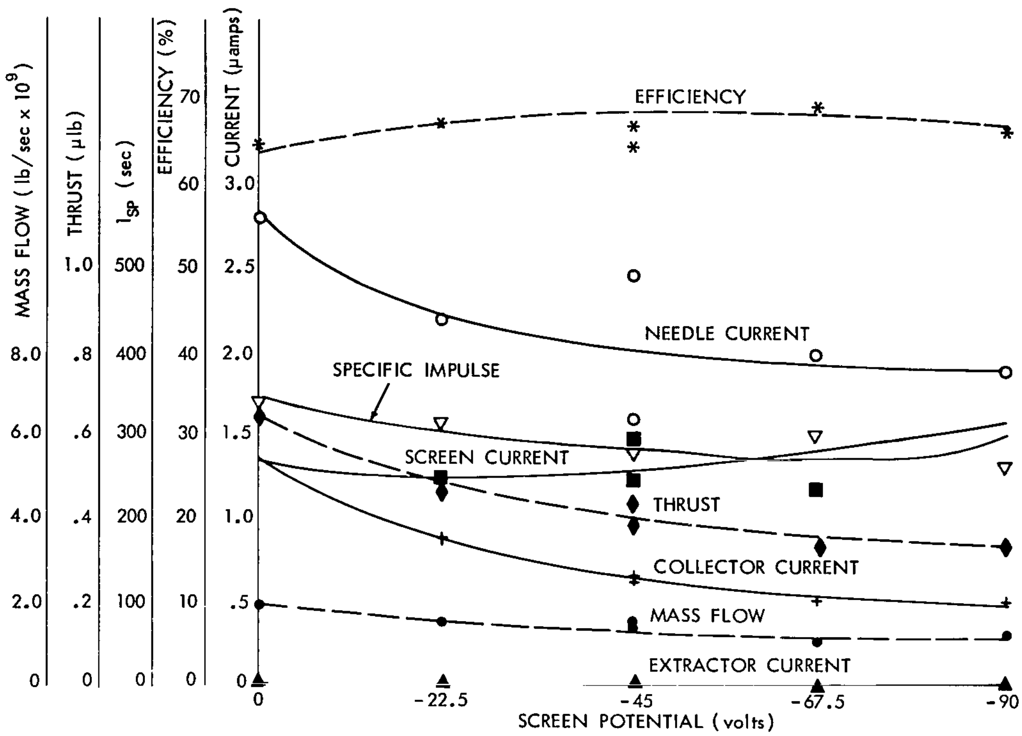

Figure 6—Test 20P curves (screen stand-off = 1 inch).

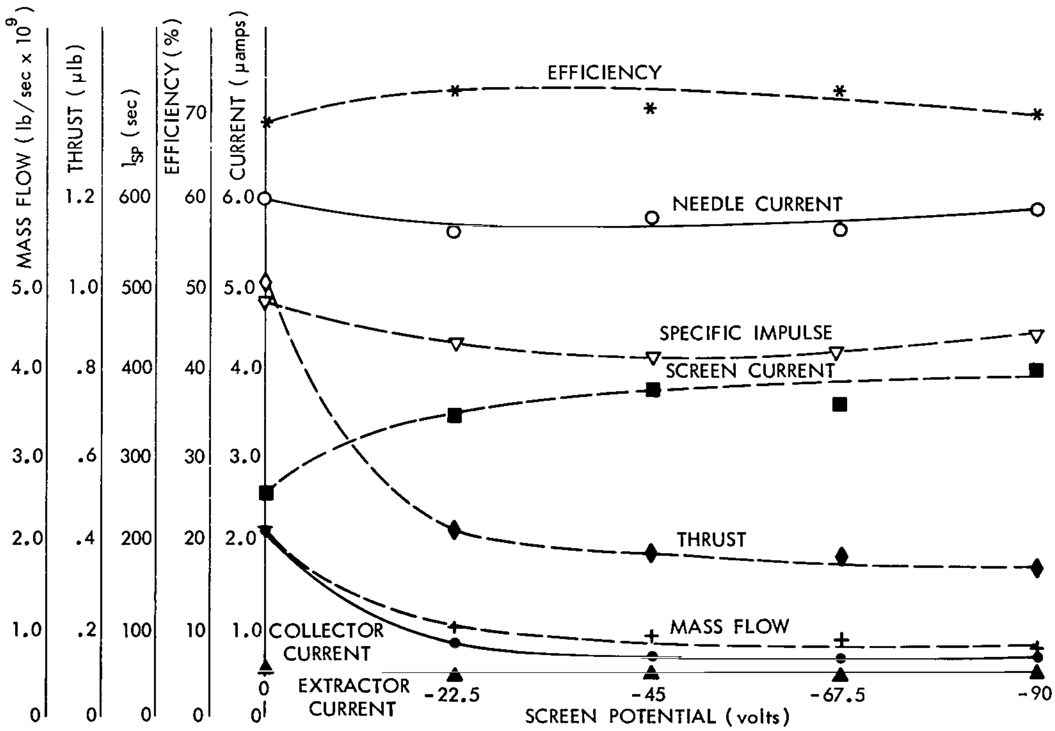

Figure 7—Test 21P curves (screen stand-off = 1/4 inch).

The needle current for test 20P decreases and for test 21P remains the same as the screen voltage becomes more negative. The decreasing needle current indicates that either the net flow of electrons into the needle or the net flow of positive particles from the needle is decreasing. A reasonable explanation for this result is that the increase in negative screen voltage decreases the secondary electron flow from the collector to the needle. Possibly this effect was obscured by the higher needle current values which were observed during test 21P.

The influence of suppression screen voltage on the needle performance parameters (computed from the TOF curves) can best be explained with reference to Figure 8, which shows the TOF traces from test 20P for suppressor screen potentials of -90v and ground. Because of secondary emission effects, as noted previously, the steady state collector current with a suppressor screen voltage of -90v is less than that with the screen at ground potential. After the zap, however, the faster colloid particles discharge to the collector, and secondary electron effects become less and less significant. Thus the two curves in Figure 9 eventually coincide, with the total current decay time being the same.

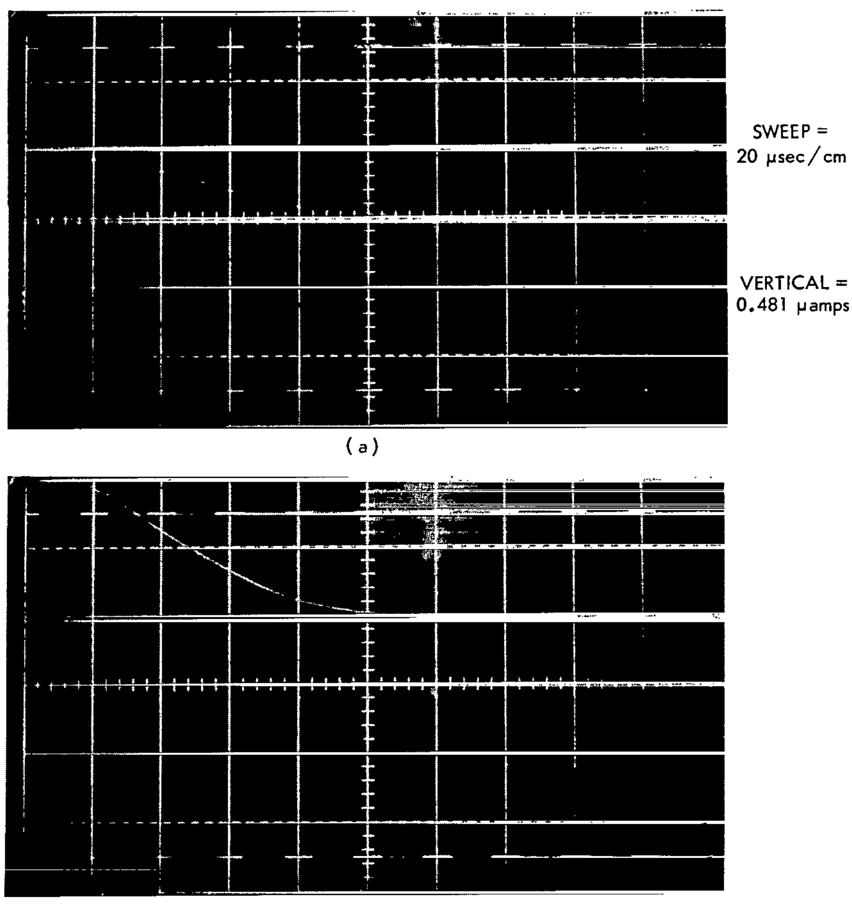

Figure 8—TOF curves of test 20P for screen potentials of (a) V_{scr} = -90v and (b) V_{scr} = ground.

In the TOF data reduction computations,

$$m \propto \int it\,dt \;.$$

It is clear from Figure 9 that m decreases as the screen voltage becomes more negative. This variation is illustrated in Figures 6 and 7.

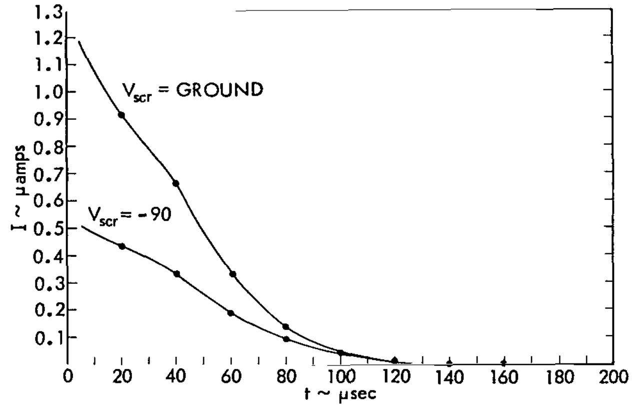

Figure 9—Comparison of TOF curves of test 20P for screen potentials of -90v and ground.

The variation of the total flow with screen voltage depends on the ratio I_N/I_c and thus is difficult to anticipate. From Table 2 it is seen that the maximum variation of the calculated m is 35 percent (with respect to its maximum value) for test 20P and 19 percent for 21P. (It is possible that some of this variation results from a change in the needle tip configuration due to erosion during the test.)

The thrust due to the particles that reach the collector is proportional to

$$\int i\,dt \;.$$

Hence the calculated value of T would be expected to decrease as the suppressor screen becomes more negative. Again this relationship is illustrated in Figures 6 and 7.

The total thrust is equal to $(I_N/I_c)T$. From Table 2, the maximum variation of the calculated value of thrust with suppressor screen potential is found to be 35 percent for test 20P and 12 percent for test 21P.

The variation in the calculated value of specific impulse (proportional to T/m) with suppressor screen potential is also shown in Figures 6 and 7. It is seen that the maximum variation in the calculated specific impulse is 19 percent for test 20P and 12 percent for test 21P.

Finally from Table 2, the calculated beam efficiency, which depends on all of the above parameters, has a maximum absolute variation with the suppressor screen voltage of 6 percent for test 20P and 4 percent for test 21P.

It was concluded from the above tests that the suppressor screen stand-off distance should be 1/4 inch and the negative voltage should be at least -22v. This will ensure that the secondary electron emission from the collector is suppressed. Furthermore, judging from Figure 7, the calculated values of the performance parameters will have reached essentially their final values. Thus if there is an error due to secondary emission effects, it is at least constant for a screen potential of -22v or greater (negatively).

The relatively small variation of specific impulse and efficiency with screen voltage is encouraging. From these tests it appears that the calculation of these two parameters may not be greatly influenced by secondary electron effects. It should be noted, however, that as thruster configurations are changed a check will be made periodically to be certain that maximum secondary suppression is being maintained.

Carbon Coating Tests

In an attempt to prevent secondary electron emission in the vacuum chamber, two tests (41P and 43P) were conducted with the suppressor screen and rear assembly coated with Aquadag (carbon dissolved in water).

Examination of the TOF curve obtained in test 41P showed no significant reduction in the positive overshoot. Furthermore, needle performance during the test was as erratic as during test 40P, which was run under the same operating conditions but without the Aquadag.

During test 43P negative collector currents were observed. Various tests were run to determine the reason for this strange occurrence. One was to keep everything constant except screen voltage, which was increased negatively to -90v in four steps. During this progression, it was observed that the collector current became increasingly negative. It thus appeared that the negative current was caused by secondary electrons bombarding the collector. Another test (44P) was run after removing all traces of Aquadag and cleaning the chamber. (It should be noted here that the Aquadag had become quite hard and flaky.) This test showed that the collector currents were now reading positive and normally. Apparently either the Aquadag degraded, causing excessive electrons to be emitted, or a current leak developed between the screen and collector. It was concluded that the use of Aquadag had no beneficial effects.

Auxiliary Plate

One test conducted with an auxiliary extractor plate attached to the needle holder and maintained at the needle potential, was an attempt to reduce secondary electron effects by having the plate serve as an electron collector. The TOF curves obtained in this test (42P) had no positive overshoots with the same operating conditions as test 41P. It would appear, therefore, that the auxiliary plate was effective in suppressing secondary electron effects. Because of the unknown effect of the plate on the electric field around the needle, however, this method was not adopted as part of the test procedure.

Screen Liner

Another test was conducted with a grounded metal screen liner in the vacuum chamber, with provisions for voltage biasing (24P). Extremely erratic performance occurred during this test at all liner biasing voltages, and a TOF curve could not be obtained. It was concluded that the screen liner was detrimentally affecting the secondary emission problems.

Extractor Inner Diameter Variations

Tests 39P and 40P were conducted under the same conditions except that the extractor used in 39P had a .437-inch i.d. while that used in 40P had a .274-inch i.d. The purpose of this was to determine whether performance could be improved by getting better field shaping with the smaller i.d.

Results of the testing showed that the smaller i.d. extractor improved specific impulse; however, performance was erratic and a positive overshoot of the TOF curve resulted. The larger i.d. extractor produced more stable results with no TOF overshoot.

Test 44P was a rerun of 39P to determine whether the feed pressure and voltage could be changed to levels such that the specific impulse and ACMR would return to those values attained in test 40P. As shown by the results in Table 2, both the ACMR and specific impulse obtained by this test were higher than those obtained in either test 39P or 40P.

From the above results it was concluded that the smaller extractor size did not significantly improve specific impulse or ACMR. Moreover, the erratic performance which results from running the smaller extractor made its use unwise.

It is interesting to consider Figure 10, obtained from Reference 4, which is a plot of a function that, for a given high voltage, is proportional to the field force on the needle tip, versus the extractor diameter-to-needle diameter ratio, as obtained from a theory presented in the reference. The two extractor sizes tested in this program fall on the asymtotic portion of the curve. Thus according to this theory no change in performance (ignoring secondary emission effects) would be expected between these two extractor sizes.

Extractor Voltage Variations

Test 46P was conducted to determine the effect of varying extractor voltage while holding all other operating parameters constant. Figure 11, which is a plot of specific impulse versus extractor voltage, shows the results of this test. It can be concluded from Figure 11 that the

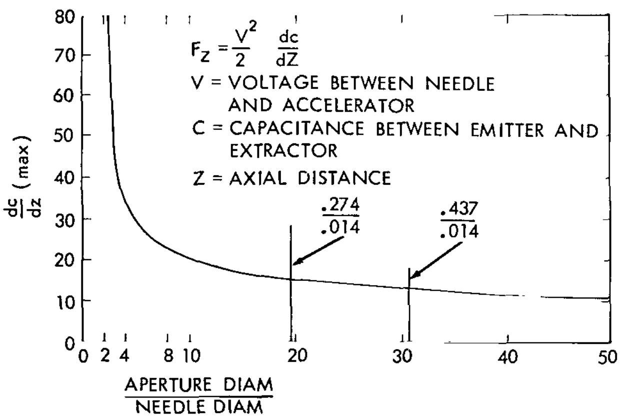

Figure 10—Force function vs aperture-to-needle diameter ratio (curves from Reference 4).

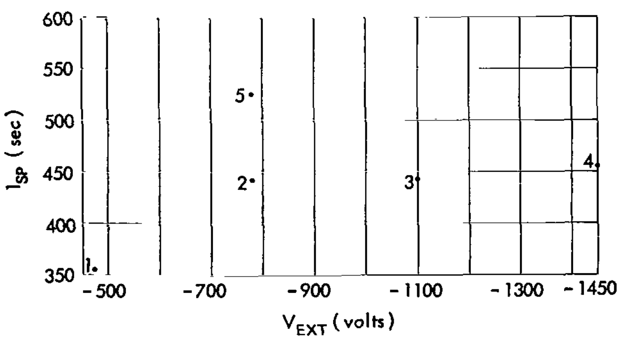

Figure 11—Specific impulse vs extractor voltage for test 46P.

variation in specific impulse which occurred is probably due to a change in needle tip shape caused by deposit build-up, rather than being related to the change in extractor voltage, as evidenced by the increase of specific impulse (and also the decrease of flow rate with time). See Table 2.

Propellant Variations

A series of tests was carried out, the object of which was to determine the performance characteristics of several different propellant combinations. A summary of the results of these tests is contained in this section.

All of the propellant variation tests up to and through test 38P were run with a needle having a rim radius of approximately .001 inch, while a .0001-inch rim radius was employed in later testing. As will be discussed later, stability problems and needle tip deposits were considerably reduced with the .0001 inch radius design.

Hydrochloric Acid-Glycerol Tests

Test 29P employed a propellant consisting of 2.5 ml of a 38-percent hydrochloric acid solution and 100 ml of glycerol. The resistivity of the propellant measured 3100Ω-cm at 25°C before the degassing procedure and 7100Ω-cm after the test. The test was run without fully dehydrating the propellant, because the high partial pressure of HCl made dehydration without driving off a substantial amount of HCl extremely difficult. Sporadic collector current pulsing, with a zero d.c. level, was observed during this run. The test was eventually terminated because of the collection of bubbles at the needle inlet.

Test 30P was run with a propellant consisting of 34 ml of a 38-percent hydrochloric acid solution and 100 ml of glycerol. The resistivity of the propellant before degassing measured 88Ω-cm at 25°C. Various values of positive and negative needle voltage (in the 4- to 5-kv range) were applied during this test, but in all cases erratic performance and sporadic pulsing of the collector current were observed. In addition, severe erosion of the needle occurred, as shown in Figure 12, even though the total duration of the test was only 20 minutes.

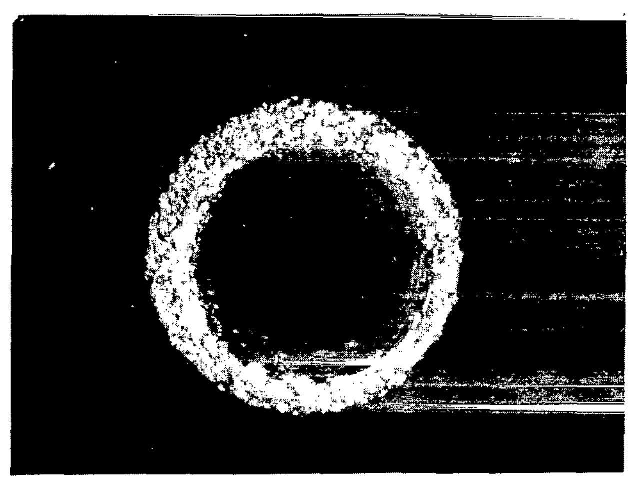

Figure 12—Needle tip after HCl-glycerol test (30P).

Sulfuric Acid-Glycerol Tests

A propellant of 10.5 ml of a 98-percent sulfuric acid solution and 100 ml of glycerol was used for test 31P. The resistivity was 450Ω-cm at 31°C before degassing and 800Ω-cm at 26°C after the test. Performance during these runs was very erratic for both positive and negative voltages, with collector current pulses in the range of 12 microamps. Also, at negative needle voltages a bright glow was observed at the needle tip. During this test (31P), as in the tests with the hydrocholoric acid-glycerol propellant combination, severe needle tip erosion occurred (Figure 13).

Test 32P was run with a propellant combination of 2 ml of a 98-percent sulfuric acid solution and 250 ml of glycerol. The resistivity before degassing was 3600Ω-cm at 26.5°C. The steady state collector current for this test was approximately .05 μamps at +6 kv and, again, was extremely erratic. It is believed that some water probably remained in the propellant after the degassing process, causing this erratic performance. This hypothesis is suggested by the observation that the feed line system pressure was pumped down to only 55 microns Hg before the test instead of the usual 15 to 20 microns. Examination of the needle after the test showed indications of erosion (Figure 14), but the degree of erosion here was much lower than that of tests 30P and 31P. Since the needle was not run at negative potential during this test, this reduced erosion suggests that most of the erosion in the previous tests occurred during operation at negative needle voltages, when the bright glow at the needle tip was observed.

Test 33P was run with the same propellant batch as 32P but with the feed line pressure pumped down to 15 microns Hg before the test. The resistivity measured after the test was 3400Ω-cm at 26°C. Erratic performance again occurred during this test; however, it was possible to obtain a TOF trace (see Table 1). There was no needle erosion during this test, again indicating that the erosion during tests 30P and 31P occurred primarily at negative needle voltage. A micro-photograph of the needle tip taken after test 33P is shown in Figure 15.

Figure 13—Needle tip after H_2SO_4-glycerol test (31P).

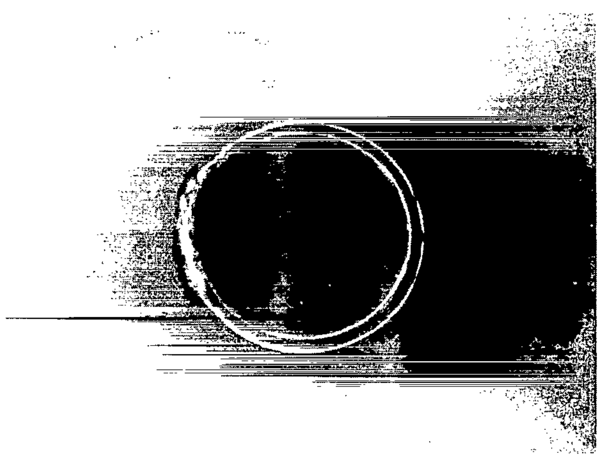

Figure 14—Needle tip after H_2SO_4-glycerol test (32P).

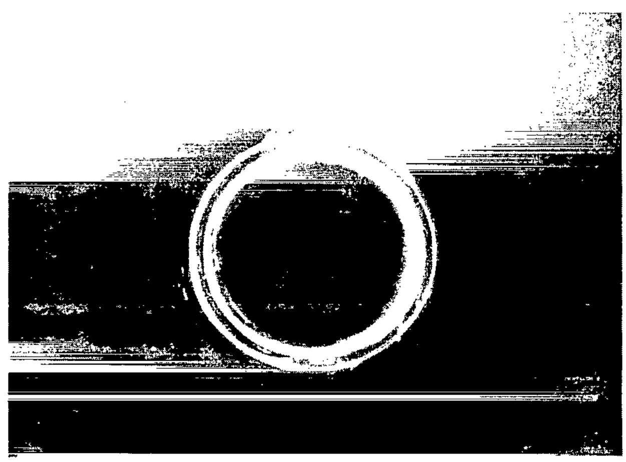

Figure 15—Needle tip after H_2SO_4-glycerol test (33P).

Sodium Hydroxide-Glycerol Tests

Test 34P employed a solution of 1 gram NaOH in 100 ml of glycerol. The resistivity of this solution was 4780Ω-cm at 26°C before degassing and 4300Ω-cm at 28°C after the test. Except for some initial instabilities, this test was fairly stable; the performance parameters are shown in Table 2. Since the specific impulse of this propellant combination was low, it was decided to run the next test (35P) with a higher concentration of NaOH in the propellant.

Before discussing test 35P in detail, it may be simply noted that one experiment tried during this test was to move the needle in such a way that it was visible in front of the extractor in one case and behind it in the other. No difference in steady state collector current was observed.

Test 35P employed a propellant solution of 2.3 grams NaOH in 100 ml of glycerol. The resistivity of the solution of the solution measured 2130Ω-cm at 28°C before the degassing process and 4250Ω-cm at 23°C after the test. The thruster exhibited fairly stable operation with this propellant. Consequently, the needle was operated for a period of about 6 hours at various combinations of feed pressure and voltage. As shown in Table 2, the specific impulses obtained during this period ranged from 211 to 583 seconds.

Examination of the needle after the test showed a collection of crystalline particles at the needle tip, as shown in Figure 16. It was thought that these particles consisted of sodium hydroxide that precipitated out of the solution as evaporation of glycerol occurred at the needle tip. If this were true, it would be expected that at lower flows, and hence larger needle tip residence time per fluid particle, the rate of sodium hydroxide precipitation would be greater than at higher flows. It was therefore decided to conduct two sodium hydroxide-glycerol propellant tests for the same length of time but with different feed pressures. The needle tip would then be examined to determine whether particle precipitation occurred to a greater degree during the lower feed pressure test.

Figure 16—Needle tip after NaOH-glycerol test (35P).

Tests 36P and 37P were both run with the 2.3-gram NaOH-100 ml glycerol propellant combination, with a resistivity before degassing of 3100Ω-cm at 24°C. The same needle was used for both tests and was cleaned before each. Examination of the needle tip after these two tests showed the same deposit as in Figure 16 but to a lesser degree, with no discernable difference in the amount of precipitate between the two tests. Thus the amount of precipitate left on the needle was not a visible function of the propellant flow as previously speculated. The composition of the precipitate remained unknown.

Sodium Iodide-Glycerol Test

As Table 2 shows, a number of tests with the .001-inch radius needle were run with a NaI-glycerol propellant combination. Some of the more significant tests were tests 26P through 28P, which showed that increasing the concentration of NaI increases the specific impulse but results in less stable operation. In general NaI resulted in better stability and performance than the other propellant combinations.

At the end of the propellant variation testing, it was obvious that sulfuric acid and hydrocholoric acid were not very good propellant doping agents. The sodium hydroxide-glycerol propellant resulted in fairly stable performance with a reasonably good specific impulse for the needle voltage applied, but because of the needle tip precipitation problem it was decided to use the sodium iodide-glycerol combination as the propellant for subsequent needle tests.

Needle Geometry Variations

Figure 17 shows the approximate dimensions of the three different needle geometries tested during this program. In comparing the performance of these configurations, it was concluded that the specific impulse and ACMR of both the internally tapered and externally tapered designs were superior to those exhibited by the straight, blunt needle, with little difference in beam efficiency. For example, both tests 47P (internal taper) and 48P (external taper) exhibited a specific impulse of about 870 seconds, which was higher than could be achieved during any of the blunt (tip radius .001 inch) needle tests (13P-38P). This result is expected since the smaller needle tip radius of the tapered versions (.0001 inch) produces a larger electric field concentration at the tip. The collector current for both the internally and externally tapered needle tests (39P, 44P, 48P) was more stable than during any of the .001-inch needle tests.

There was no significant difference in performance or stability between the internally- and externally-tapered needles; however, pre- and post-test cleaning of the needle was easier with the externally-tapered design.

Since generally better performance was obtained with the thin-rimmed needles, it should be noted that, some of the particle precipitation problems associated with the earlier sodium hydroxide-glycerol tests possibly could have been reduced or eliminated by using these needle geometries. However, because of the generally successful performance of the sodium iodide-glycerol propellant in these tests, no additional propellant evaluation testing was conducted.

Needle Material

The following needle materials were tested during this program:

Material	Tests
Stainless steel	1P-13P (Results not shown in Table 2)
Hastelloy C	14P-20P
Platinum	21P-26P
Platinum — 10% iridium	27P-48P

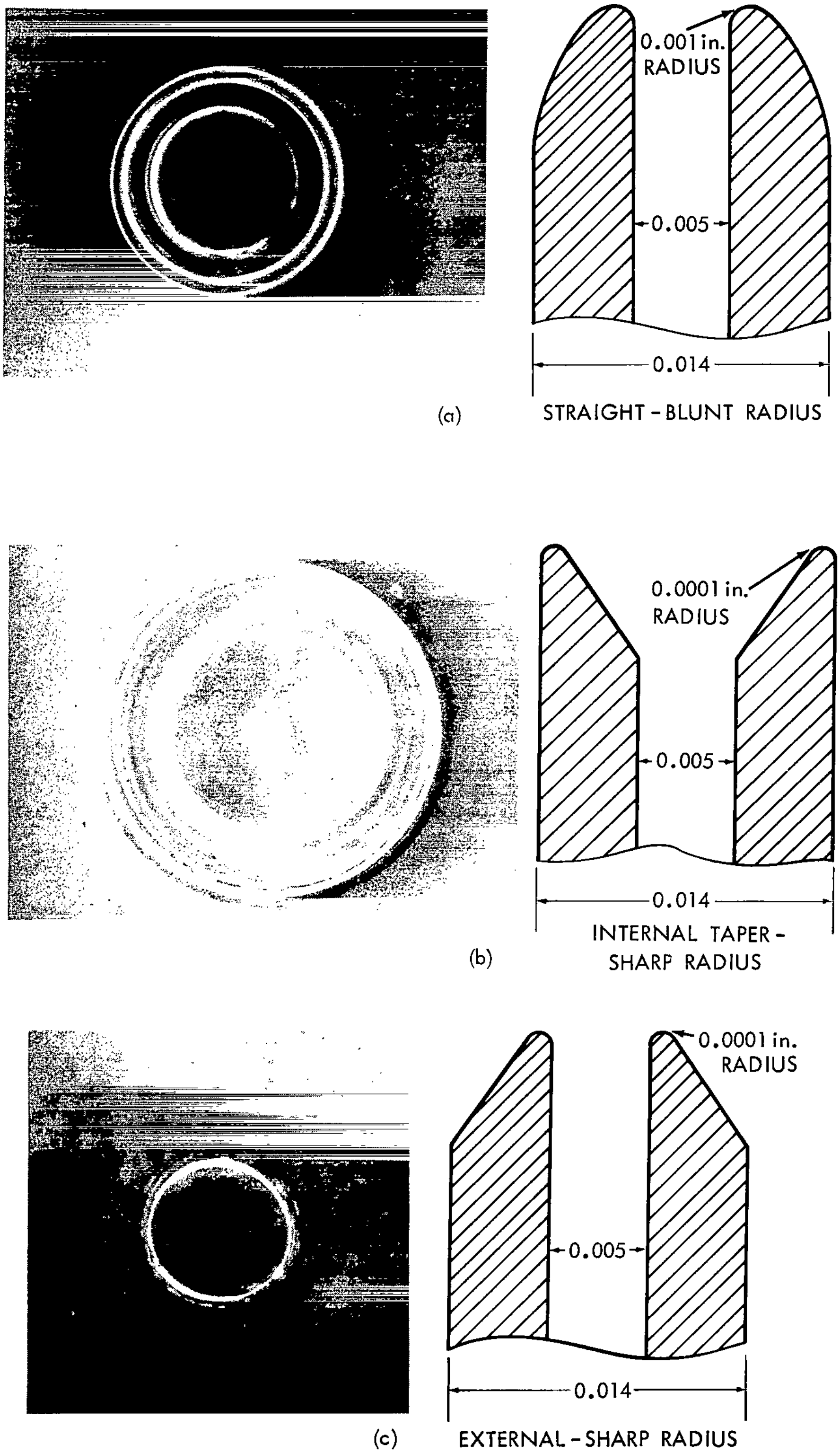

Figure 17—(a) Straight, blunt needle geometry; (b) internally tapered sharp needle geometry; and (c) externally tapered sharp needle geometry.

The stainless-steel needles exhibited severe needle-tip erosion and pitting when used with the sodium iodide-glycerol propellant combinations. The use of stainless-steel needles was therefore abandoned early in the program. Hastelloy C was then employed as a needle material. Erosion again occurred with the sodium iodide-glycerol combinations but at a reduced rate and with no pitting. In addition, the Hastelloy C needles were run for 24-hour periods with reasonably good performance.

Tests 21P through 26P, conducted with a pure platinum needle, resulted in little or no erosion of the needle tips; however, the softness of pure platinum made needle fabrication extremely difficult and needle damage a likely occurrence during handling. For this reason, the remainder of the tests were run with a platinum 10-percent iridium alloy, which was considerably easier to work and equally resistant to erosion. Tests 27P to 48P resulted in little or no erosion of the needle tip, except when an acid-glycerol combination was used as a propellant, as previously described.

MATERIAL TESTING

An analogy can be made between the process by which charged particles are formed and moved from thruster to collector and an electrochemical process. Figure 18 shows schematic representations of the colloid firing process and an electrochemical process. In particular, the propellant in the colloid thruster can be considered analogous to the chemical medium in the electrochemical process. In Figure 18a the anode is taken as the needle and the cathode as the collector; in Figure 18b the anode is the needle metal to be tested and the cathode is a stable metal such as platinum. The transfer medium is the propellant combination to be tested.

Considering only stable operating conditions of the needle setup (i.e., no arcing or tip glowing), it was found that propellant breakdown and needle erosion performed proportionately to the electrochemical analogy. Because the electrochemical current flow is much higher than the analogous needle current flow (milliamps vs microamps), erosion and propellant breakdown were more rapid; it was therefore decided to use this method to evaluate the stability of various metals in assorted propellant combinations. The results are presented in Table 3.

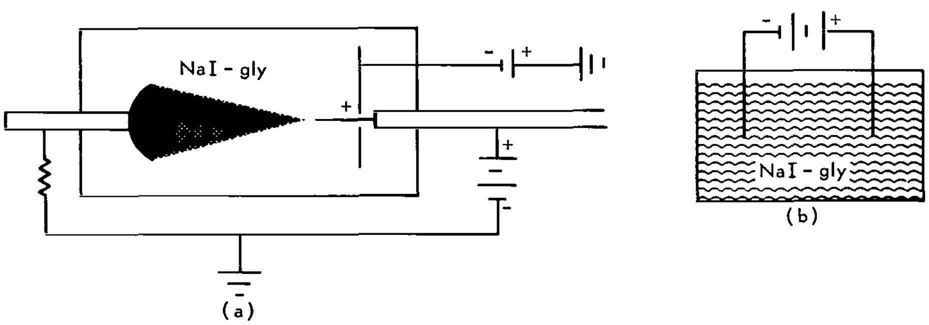

Figure 18—Schematic representation of colloid firing and electrochemical processes.

Table 3

Summary of Electrochemical Erosion Tests.

Anode	Cathode	Electrolyte	Conditions	Results
Gold plated—20 CB S.S.	Platinum	2 ml H_2SO_4— 250 ml glycerol (A)	20 vdc for 3 hrs	Black deposit collected on gold but washed off easily. No apparent erosion.
Gold plated—20 CB S.S.	Platinum	20 gm NaI— 100 ml glycerol (B)	20 vdc for 1 hr	Heavy deposit of iodine on gold. Considerable erosion.
Gold plated—20 CB S.S.	Platinum	2.3 gm NaOH— 100 ml glycerol (C)	20 vdc for 1 hr	Black deposit collected on gold but washed off easily. No apparent erosion.
Rhodium plated brass 100-μin. plate 200-μin. plate 500-μin. plate	Platinum	(B)	20 vdc for 3 hrs	No apparent erosion under 750× magnification.
Rhodium plated brass 100-μin. plate 200-μin. plate 500-μin. plate	Platinum	(A)	20 vdc for 3 hrs	No apparent erosion under 750× magnification.
Rhodium plated brass 100-μin. plate 200-μin. plate 500-μin. plate	Platinum	(C)	20 vdc for 3 hrs	No apparent erosion under 750× magnification.
Platinum plated— 20 CB S.S.—100-μin. plate	Platinum	(A)	Approx. 20 vdc	No apparent erosion.
Platinum Plated— 20 CB S.S.—100-μin. plate	Platinum	(C)	Approx. 20 vdc	No apparent erosion.
Platinum plated— 20 CB S.S.—100-μin. plate	Platinum	(B)	Approx. 20 vdc	Iodine collected on platinum but washed off easily. No apparent erosion.

Although both rhodium and platinum exhibited excellent corrosion-erosion resistance, it was decided to use platinum in the needle and in the future annular slit configurations because of its availability and good working characteristics. Rhodium is very brittle and micro-cracks tend to form easily. No extensive tests were run on stainless steel, Hastelloy, 20 CB, or other similar metals because periodic electrochemical tests on these (using them as anodes with a platinum cathode) showed very rapid erosion.

ANNULAR SLIT DESIGN AND PRELIMINARY TESTS

Early in this program considerable thought was given to the various types of configurations that could be used to obtain the high thrust and performance desired.

It is appropriate to state at this time the reasons for and advantages of attempting to develop a single high-thrust unit rather than depend on the present multiple needle arrays. Assuming that it is possible to get 3 micropounds of thrust per needle, it would require more than 30 needles to get 100 micropounds. To get higher thrusts one would require a correspondingly greater number of needles. The fact that all of these needles must somehow be permanently attached to a common feed system, while each must be surrounded by an extractor and all must be equidistant from each other, presents considerable technological problems and difficulties. If one needle became damaged, it would be extremely difficult to replace it without disturbing or damaging the surrounding needles. Extreme care must be exercised in the handling of such a unit to prevent accidental damage.

A single flow area thruster (e.g., the annular slit), capable of producing the required thrust and exhibiting the desired overall performance, has the obvious advantages of simplicity and convenience. If the rims should become damaged, they can be repolished easily. A linear and an annular slit thruster were therefore designed and built (Figure 19).

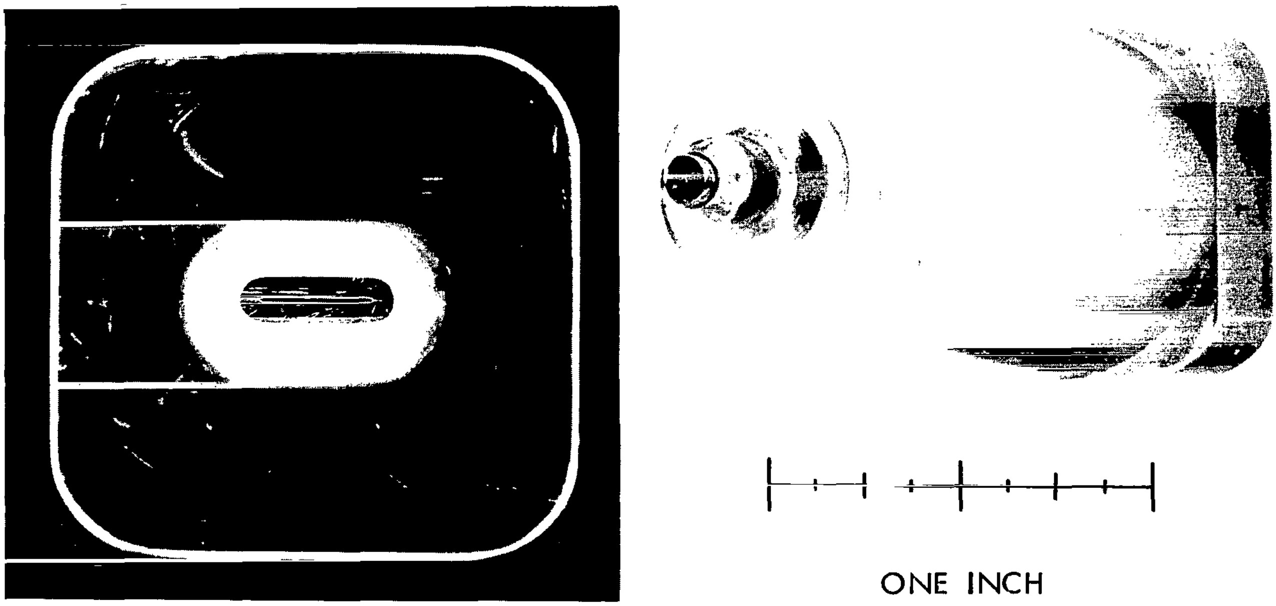

(a) (b)

Figure 19—Slit configurations; (a) linear slit thruster and (b) annular slit thruster.

The annular slit thruster was chosen as the configuration to be tested first following conclusion of the needle tests, because its basic slit geometry provides for uniform and uninterrupted electric field intensity lines. This should provide an inherently more uniform spray pattern and hence better general performance characteristics. The following are the basic requirements on which the annular slit design (Reference 7) is based.

$$T = 150 \times 10^{-6} \text{ lb};$$

$$I_{sp} = 900 \text{ sec};$$

$$q/m = 3000 \text{ coul/kg} \; ; \text{ and}$$

$$m = \frac{T}{I_{sp}} = \frac{150 \times 10^{-6}}{900} = 1.67 \times 10^{-7} \frac{\text{lb}}{\text{sec}} \, .$$

This design was based on the practicality of the smallest machinable dimensions for R (inner radius) and h (slit width). R was chosen as .0400 inch. Calculations based on the required $\dot{m}$ resulted in

$$R_0 = .0422 \text{ in.} \; ;$$

$$\frac{\Delta P}{L} = 2 \, .$$

For L = 1.5 in.,

$$\Delta P = 3 \text{ psi} \, .$$

See Figure 20 for definitions of R, R_0, h, and L.

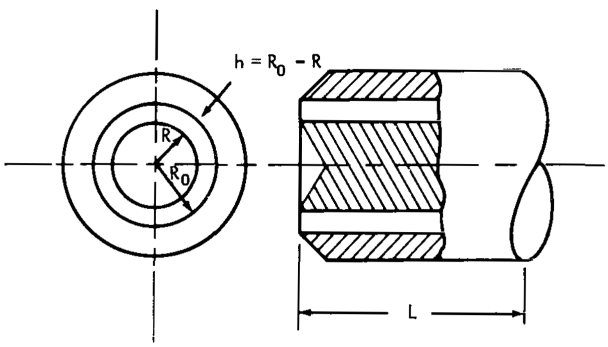

Figure 20—Annular slit thruster geometry.

After the annular slit was fabricated, its outer and inner surfaces were plated with 100×10^{-6} inches of platinum. Under this were base platings of nickel and gold amounting to about 70×10^{-6} inches. Before testing the thruster, the rims were polished to a rim thickness of about .0001 inch.

There was no problem with polishing the inner rim; however, when the outer rim was polished, it was found that hollow bubbles of platinum were coating it, as shown in Figure 21. As polishing proceeded, these bubbles came off, exposing the base metal (20 CB), as shown in Figure 22.

Figure 21—Outer rim platinum plating, polishing not complete.

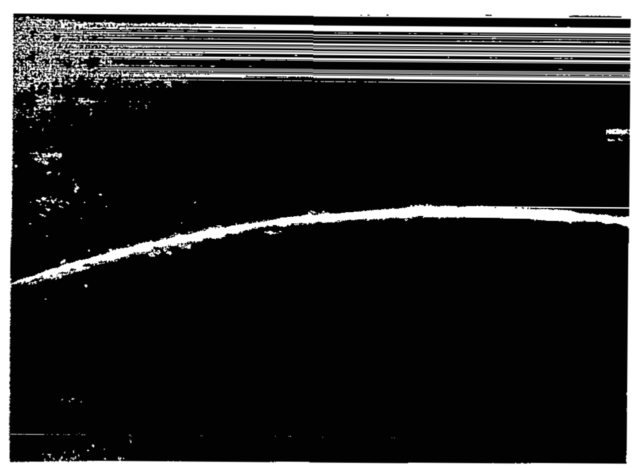

Figure 22—Outer rim platinum plating after polishing.

The GSFC Plating Section was consulted as to why this discrepancy in plating characteristics between outer and inner rims existed. Their explanation was that a "thief" was used around the inner rim surface, thus reducing the current density and the rate of platinum plating. However, on the outer rim no "thief" was used and, as a result, a large current density was present which allowed too rapid a rate of platinum and base metal plating.

With this thruster, preliminary tests were run with a NaI-glycerol propellant solution to prove operational feasibility. Results were very encouraging although the thrust and flow were below design values. Table 4 presents a summary of these initial tests.

Table 4

Summary of Initial Tests on Annular Slit.

Test Number	Propellent	P_f mm Hg	V_S (kv)	V_{EXT} (volts)	V_{SCR} (volts)	I_0 (μamps)	I_S (μamps)	I_{EXT} (μamps)	ACMR	q/m	$\dot{m}$ $\left(\frac{lb}{sec}\right)$ $\times 10^{-8}$	$\frac{I_S}{I_0}\dot{m}$ $\times 10^{-8}$	T (μlb)	$\frac{I_S}{I_0}T$ (μlb)	I_{SP} (sec)	η_b (%)
A.S. 3-2	20 g NaI 150 ml gly.	128	20	-473	-45	12.8	150	12	2620	1700	1.07	12.5	9.0	105.5	840	64.9
A.S. 8-1	35 g NaI 117 ml gly.	55	20	-473	-45	13.1	175	4	5079	2852	.569	7.6	6.2	83	1085	56.1
A.S. 9	35 g NaI 117 ml gly.	113	20.5	-473	-45	13.3	163	6	4813	2643	.609	7.45	6.36	78	1045	54.9

FUTURE PROGRAMS

Having proven feasibility of the annular slit thruster, further efforts in this area will be directed towards improving general overall performance so as to more closely approach initial design goals. The programs as discussed in this section are those considered necessary in order to improve performance.

Vertical Mounting

It has been decided to mount the thruster vertically for future testing rather than horizontally, as in the initial tests, because during these tests it was observed that propellant spray collected on the bottom segment of the glass vacuum "T" section. No propellant deposit of this order was noted in the top section of the glass "T." Vertical mounting would also eliminate the gravity effect on the meniscus, since its plane would be parallel to the horizontal. In the horizontal position, gravity may cause the meniscus to collect at the bottom thus giving poor velocity distribution to the beam.

Optimization of Present Configuration

Testing will be directed towards optimizing the extractor configuration and its location with respect to the firing surface. In conjunction with this, tests will be conducted to reduce beam divergence through the use of focusing devices.

Sputter-Plated Thruster

A thruster configuration identical to the one being discussed here is presently having its rims plated with platinum by an RF sputtering technique. This method is supposed to have the advantage of being able to plate a very thin layer of platinum on surfaces of extremely small radii without causing the usual electrochemical problems of excessively thick and nonuniform edges. In fact, it is claimed that edges plated in such a manner will have radii more uniform than before plating. If this result is obtained, it may be possible to get good performance parameters at considerably lower thruster voltages.

Propellant Optimization

During the extensive testing of needles and the initial testing of the annular slit thruster, wide performance variations were noted between the use of NaI and acids as the dopant in glycerol. Although NaI contributed to a more stable performing propellant, the acids produced a more active propellant. This activity of the acids contributed to erratic collector currents with very high peak currents.

It is possible that a three-component propellant (e.g., NaI, H_2SO_4, and glycerol) in the right proportions would yield stable performance with higher collector currents. Of course there are many possible combinations with varying proportions of each component. In addition, an attempt could be made to obtain a different base component which would have greater viscosity stability with temperature variations than does glycerol.

This particular investigation, with the great number of combinations possible, would in itself constitute a very time consuming program.

CONCLUSIONS

The scope and depth of the needle testing program were varied enough to make possible a complete familiarization with the technology of electrostatic spraying. From the results of the many tests conducted, an understanding of the behavioral characteristics of secondary electron emission inside the vacuum chamber was developed. In addition, material erosion characteristics were studied. The ability to test several propellant combinations with varying concentrations created a greater understanding of propellant performance characteristics and their effects on needle material. The testing of various needle tip geometries provided data on the effects of rim radius and shape on performance.

With this information and experience, it was possible to proceed into the annular slit program with a basic understanding of the principle of electrostatic propulsion and the ability to make sound engineering judgments in testing and design areas. It was also possible to define the areas in which further research and development are required in order to optimize the annular slit thruster design.

ACKNOWLEDGMENT

The authors wish to express their appreciation to Mr. William Burton who so ably set up and ran the colloid laboratory test facility and who was instrumental in arriving at design concepts, solving testing problems, and making innumerable other valuable contributions to the overall program.

Goddard Space Flight Center
National Aeronautics and Space Administration
Greenbelt, Maryland, February 20, 1968
120-26-02-01-51

REFERENCES

1. Cohen, E., "Experimental Research to Determine the Feasibility of a Colloid Thruster," Air Force Aero Propulsion Laboratory, AFAPL-TR-65-72, 1965.

2. Wineland, S., Burson, W., and Hunter, R. E., "The Electrohydrodynamic Generation of Charged Droplet Beams," Air Force Aero Propulsion Laboratory, Wright-Patterson Air Force Base, Ohio, AFAPL-TR-66-72, August 1966.

3. Beynon, J., et al., "Present Status of Colloid Microthruster Technology," AIAA Paper 67-531, 1967.

4. Perel, J., "Electrodeless Particle Thruster," Air Force Aero Propulsion Laboratory, Wright-Patterson Air Force Base, Ohio, AFAPL-TR-67-106, October 1965.

5. Cohen, E., "Research on Charged Colloid Generation," Air Force Aero Propulsion Laboratory, Wright-Patterson Air Force Base, Ohio, APLTDR 64-75, June 1964.

6. Schlichting, H., "Boundary Layer Theory," New York: McGraw-Hill, 1955.

BIBLIOGRAPHY

Burson, W., "Research on Electrohydrodynamic Charged Droplet Beams," Air Force Aero Propulsion Laboratory, Wright-Patterson Air Force Base, Ohio, AFAPL-TR-67-109, October 1967.

Pfeifer, R., "Parametric Studies of Electrohydrodynamic Spraying," Engineering Experiment Station, Univ. of Ill., Report No. CPRL-4-65, 1965.

Appendix

List of Symbols

m = mass flow as measured at the collector

g_0 = acceleration of gravity

v = velocity

T = thrust as measured at the collector

I_{sp} = specific impulse

q/m = SMR charge to mass ratio

I_c = collector current

I = needle or slit currents (use N or S subscript)

η_b = beam efficiency

V = needle or slit voltage (use N or S subscript)

V_{ext} = extractor voltage

P_f = feed pressure

P_t = thruster power

d = time of flight distance

I_0 = TOF collector current at time = 0

t_f = TOF time at current = 0

I_{ext} = extractor current

I_{scr} = screen current (if used)

ACMR = average charge to mass ratio

$\frac{I_N}{I_C} T$ = total thrust

$\frac{I_N}{I_C} m$ = total mass flow

NASA-Langley, 1970 —— 28

NATIONAL AERONAUTICS AND SPACE ADMINISTRATION
WASHINGTON, D.C. 20546

OFFICIAL BUSINESS

FIRST CLASS MAIL

POSTAGE AND FEES PAID
NATIONAL AERONAUTICS AND
SPACE ADMINISTRATION

03U 001 53 51 3DS 70033 00903
AIR FORCE WEAPONS LABORATORY /WLOL/
KIRTLAND AFB, NEW MEXICO 87117

ATT E. LOU BOWMAN, CHIEF,TECH. LIBRARY

POSTMASTER: If Undeliverable (Section 158 Postal Manual) Do Not Return

"The aeronautical and space activities of the United States shall be conducted so as to contribute . . . to the expansion of human knowledge of phenomena in the atmosphere and space. The Administration shall provide for the widest practicable and appropriate dissemination of information concerning its activities and the results thereof."

—NATIONAL AERONAUTICS AND SPACE ACT OF 1958

NASA SCIENTIFIC AND TECHNICAL PUBLICATIONS

TECHNICAL REPORTS: Scientific and technical information considered important, complete, and a lasting contribution to existing knowledge.

TECHNICAL NOTES: Information less broad in scope but nevertheless of importance as a contribution to existing knowledge.

TECHNICAL MEMORANDUMS: Information receiving limited distribution because of preliminary data, security classification, or other reasons.

CONTRACTOR REPORTS: Scientific and technical information generated under a NASA contract or grant and considered an important contribution to existing knowledge.

TECHNICAL TRANSLATIONS: Information published in a foreign language considered to merit NASA distribution in English.

SPECIAL PUBLICATIONS: Information derived from or of value to NASA activities. Publications include conference proceedings, monographs, data compilations, handbooks, sourcebooks, and special bibliographies.

TECHNOLOGY UTILIZATION PUBLICATIONS: Information on technology used by NASA that may be of particular interest in commercial and other non-aerospace applications. Publications include Tech Briefs, Technology Utilization Reports and Notes, and Technology Surveys.

Details on the availability of these publications may be obtained from:

SCIENTIFIC AND TECHNICAL INFORMATION DIVISION

NATIONAL AERONAUTICS AND SPACE ADMINISTRATION

Washington, D.C. 20546